

# RSC Advances



This is an *Accepted Manuscript*, which has been through the Royal Society of Chemistry peer review process and has been accepted for publication.

*Accepted Manuscripts* are published online shortly after acceptance, before technical editing, formatting and proof reading. Using this free service, authors can make their results available to the community, in citable form, before we publish the edited article. This *Accepted Manuscript* will be replaced by the edited, formatted and paginated article as soon as this is available.

You can find more information about *Accepted Manuscripts* in the [Information for Authors](#).

Please note that technical editing may introduce minor changes to the text and/or graphics, which may alter content. The journal's standard [Terms & Conditions](#) and the [Ethical guidelines](#) still apply. In no event shall the Royal Society of Chemistry be held responsible for any errors or omissions in this *Accepted Manuscript* or any consequences arising from the use of any information it contains.

# **A Simple Method for Fabrication of Microfluidic Paper-Based Analytical Devices and on-device Fluid Control with a Portable Corona Generator**

**Yan Jiang<sup>1</sup>, Zhenxia Hao<sup>2</sup>, Qiaohong He<sup>1\*</sup>, Hengwu Chen<sup>1</sup>**

**1. Institute of Microanalytical Systems, Department of Chemistry, Zhejiang University, Zijing'gang Campus, Hangzhou 310058, China**

**2. Tea Research Institute, Chinese Academy of Agricultural Sciences**

\*Author to whom correspondence should be addressed; E-mail: heqh@zju.edu.cn;

Tel.: +86-571-88206773; Fax: +86-571-88273572

**Abstract:** This work presents a facile method for fabrication of microfluidic paper-based analytical devices ( $\mu$ PADs) and on-device fluid control with a portable, hand-held corona generator. First, filter paper was hydrophobized by coupling octadecyltrichlorosilane (OTS) to paper cellulose. Then, the OTS-coated paper, covered with a stenciled plastic mask, was region-selectively exposed to the corona by scanning the electrode tip of the corona generator along the open parts of the mask. Thus, the corona-exposed regions of the paper surface resumed its native hydrophilicity while the masked regions remained highly hydrophobic. The effect of corona treatment time on paper's hydrophilic property was investigated. Colorimetric assays of nitrite in saliva sample were demonstrated with the developed  $\mu$ PADs. A single-use 'on' valve based on wettability-switching was developed in  $\mu$ PADs. Fluid control was realized via on-site corona discharge targeted at a hydrophobic barrier design as the 'on' valve.

**Key Words:** microfluidic paper-based analytical devices; hand-held corona generator; fabrication; saliva; nitrite; fluids control

## 1. Introduction

Microfluidic paper-based analytical devices ( $\mu$ PADs), also known as lab-on-paper technology, has attracted great interest since its introduction by Whitesides and coworkers in 2007.<sup>1</sup> It has merged the advantages of conventional microfluidic chips with the features of paper substrates, and thus offers attractive merits from the very beginning of its appearance, including simplicity, inexpensiveness, biocompatibility, portability and disposability. However, the key advantage of  $\mu$ PADs is that aqueous solutions in channels could be driven by capillary wicking, thus no external pumps are required. These features make  $\mu$ PADs a fascinating technology for clinical diagnosis, food quality control and environmental monitoring,<sup>2-9</sup> especially in less-developed countries and resource-limited situations.

$\mu$ PAD construction is normally based on the principle of generating hydrophilic-hydrophobic pattern on a paper substrate to create millimeter-sized capillary channels. So far, numerous techniques for fabrication of  $\mu$ PADs have been reported, including photolithography,<sup>1, 10, 11</sup> wax patterning,<sup>12-17</sup> plasma treating,<sup>18</sup> inkjet printing,<sup>19, 20</sup> inkjet etching,<sup>21, 22</sup> plotting,<sup>23</sup> and some other techniques.<sup>24-26</sup> Photolithography was the first established method for fabrication of  $\mu$ PADs. Whitesides and coworkers relied on exposing photoresist-coated paper to UV lights to create hydrophilic channels defined by hydrophobic cured photoresist.<sup>1</sup> Our group demonstrated a novel and facile approach for fabrication of  $\mu$ PADs via silanization of paper cellulose followed by region-selective UV irradiation.<sup>10</sup> Photolithography was featured in high resolution but limited by complicated fabrication process and expensive equipment required. Wax-patterning made use of cost-effective and easily available wax to form hydrophobic pattern. Wax could be applied to paper by a variety of techniques, such as wax-printing with a printer,<sup>12-14</sup> wax-dipping with a metal mask,<sup>15</sup> wax-stamping with a metallic stamp,<sup>16</sup> and wax-screen-printing with standard emulsion-based screens.<sup>17</sup> In these wax-patterning techniques, wax-printing stood out because it allowed mass production with a simple and fast fabrication process. Unfortunately, wax-printers are also expensive. Inkjet printing was an

effective alternative to wax-printing.<sup>19, 20</sup> Inkjet etching had the unique advantage of being able to print reagents directly into testing zones. However, it had the limitation of repeated printing steps required to generate hydrophilic areas.<sup>21, 22</sup> Nie *et al.*<sup>23</sup> reported a one-step plotting method to fabricate  $\mu$ PADs by simply using permanent markers and metal templates with specific patterns.

Though  $\mu$ PADs have already experienced a quick development in fabrication techniques, limited work has been carried out to develop functional elements for fluid control within  $\mu$ PAD channels. Up to date, efforts on fluid control within channels are mostly based on three-dimensional  $\mu$ PAD (3D- $\mu$ PAD) construction. Noh and Phillips<sup>27</sup> reported controlled wicking of fluids by adjusting the wettability of channels in the *z*-direction of 3D- $\mu$ PADs. Martinez *et al.*<sup>28</sup> controlled the movement of fluids by pressing a single-use 'on' button to close a small gap between two vertically aligned microfluidic channels so that fluids were able to wick from one channel to the other. Alternatively, Li *et al.*<sup>18</sup> pre-cut the target channel into two parts and manipulated capillary flow by manually separating or joining them.

In this work, we introduce a hand-held corona generator as an effective, inexpensive and portable tool for  $\mu$ PADs fabrication. Corona discharge treatment has been exploited as an efficient surface modification method for microfluidic chips, especially PDMS chips, during chip bonding<sup>29</sup> and channel wettability patterning.<sup>30, 31</sup> To our best knowledge, no work has been reported on using a portable corona generator to build hydrophilic pattern onto paper. Furthermore, we also demonstrate the feasibility of fluid control on  $\mu$ PADs via opening single-use 'on' valves by on-site corona discharge treatment.

## 2. Experimental Section

### 2.1 Materials and Apparatus

Octadecyltrichlorosilane (OTS, 95%) was purchased from Acros Organics (Springfield, NJ, USA). Sylgard 184 silicon elastomer kit consisting of a prepolymer base and a curing agent was obtained from Dow Corning (Midland, MI, USA).

Polymethylmethacrylate (PMMA) sheet (2 mm in thickness) was purchased from Donchamp Acrylic Co., Ltd (Taixing, Suzhou, China). Filter paper (Model 203 quantitative filter paper) was from Hangzhou Xinhua Paper Industry Co., Ltd (Hangzhou, Zhejiang, China). Human saliva sample was collected from a volunteer after fasting for 2 h. Indicator solution for nitrite assay contained 50 mmol L<sup>-1</sup> sulfanilamide, 330 mmol L<sup>-1</sup> citric acid and 10 mmol L<sup>-1</sup> *N*-(1-naphthyl) ethylenediamine in 80% methanol.

A Model BD-20AC corona generator was from Electro-Technic Products Inc. (Chicago, IL, USA). Plastic masks were fabricated by AMCNC-01 carving machine (Amor Electronic Technology Co., Ltd., Guangdong, China). EPSON Perfection V300 Photo desktop scanner was used to scan the images of colorimetric assays performed on  $\mu$ PADs. Water contact angle was measured by JC 2000 C3 (Shanghai Zhongchen Digital Technic Apparatus Co., Ltd, Shanghai, China). The thickness of hydrophilic layer on filter paper was determined by XTL-20 microscope (Shanghai Pudan Optical Instrument Co., Ltd, Shanghai, China). Attenuated total reflectance Fourier transform-infrared (ATR-FT-AR) spectroscopy measurements were conducted on Nicolet Nexus 470 from Nicolet (Madison, WI, USA). X-ray photoelectron spectroscopy (XPS) measurements were carried out on VG ESCALAB MARK II from VG (UK).

## 2.2 Preparation of Mould Complex

The mould complex consisted of a top stenciled PMMA mask with channel pattern, a middle PDMS elastic pad and a bottom flat PMMA plate. The pattern of the stenciled mask was first designed with ArtCAM software and then was transformed to a PMMA sheet with the carving machine. A flat PMMA sheet was cut to an appropriate size to act as the hard bottom supporter. The middle elastic PDMS pad in 5 mm thickness was prepared by casting degassed mixture of Sylgard 184 prepolymer base and curing agent (15:1) against a flat glass.

### 2.3 Fabrication of $\mu$ PADs

The fabrication process is schematically shown in Fig. 1. Filter paper was silanized to hydrophobic in OTS-hexane solution as our previous work reported.<sup>10</sup> Briefly, filter paper was cut to an appropriate size and immersed in 0.1% (V/V) OTS-hexane solution for 5 min. Then, the paper pieces were removed from the solution and rinsed sequentially with n-hexane and water, and dried under nitrogen stream. After silanization, the OTS-coated paper was sandwiched by the mould complex as shown in Fig. 1c, and tightly clamped.

The corona was adjusted to a relatively low level to produce a stable but soft corona with minimal crackling and sparking. The electrode tip was moved in  $\sim 2$  mm proximity to the paper surface to be treated, and was scanned along the open parts of the mask for a reasonable time (depending on the area to be treated). Thus, hydrophilic pattern was built on the hydrophobic OTS-coated paper substrate.

### 2.4 Nitrite Assay on $\mu$ PADs

A flower-shaped  $\mu$ PAD with one central common reagent zone, eight channels and eight detection zones was fabricated for nitrite assay. The principle of nitrite assay is based on Griess reaction which is a common quantification method for nitrite.<sup>32</sup> During the assay, 5  $\mu$ L of indicator solution was first pipetted into the central common reagent zone. The indicator solution penetrated along eight channels into the detection zones by capillary wicking. The device was allowed to air dry under dark conditions for 5 min. Then, 0.20  $\mu$ L of blank control and serially diluted  $\text{NO}_2^-$  standard solutions with the concentration of 0.02, 0.04, 0.08, 0.16, 0.32, 0.64, 1.28  $\text{mmol L}^{-1}$  were individually pipetted into each of the 8 detection zones for color development. After standing in dark for 5 min, the  $\mu$ PAD was scanned with a desktop scanner immediately, and the collected image was converted to grayscale with Adobe Photoshop CS3. The assay was repeated three times using three  $\mu$ PADs. The calibration curve was constructed according to the average gray intensities of the standards.

Saliva sample was collected and prepared as previously reported.<sup>33</sup> Specifically, saliva was collected from a volunteer after fasting for 2 h. Then the sample was

centrifuged at 2500 rpm for 10 min at room temperature (15 °C). The supernatant was analyzed for its nitrite contents. When determine the nitrite concentration in saliva sample, a blank control solution and four standard solutions with narrower concentration range (0.02-0.12 mmol L<sup>-1</sup>) were deposited on 0 and 1-4 zones, respectively, while saliva sample was deposited on 5-7 zones. The nitrite concentration of saliva sample was read against the newly constructed calibration curve based on the standard solutions.

### **2.5 Safety Consideration**

The corona generator is safe and easy to use. However some precautions need to be observed. First, when used, the instrument will produce radio frequency which may interfere with other electronic devices such as stopwatch. So they are required be kept at least 1 m away from the generator. Second, the spark emitted from the electrode tip will be easily attracted to metal objects. Thus, metal objects such as knives should be absent within the operation area, and rings and jewelry should be temporarily removed from the operator. Last, ozone gas is generated around the tip of the electrode when the air is ionized. Therefore, the instrument should be used in areas with good ventilation.

## **3. Results and Discussion**

### **3.1 Wettability-patterning of OTS-Paper with Corona Discharge**

#### **3.1.1 Mould design**

In this work, a polymeric mould complex (as shown in Fig.1) was employed. The mould complex consisted of three layers. The top layer was a stenciled PMMA mask with channel pattern. With the help of this mask, the corona discharge could be restricted within the exposed area of OTS-paper when the electrode tip of the generator was manually scanned along the open parts of the mask, rendering the exposed parts of OTS-paper hydrophilic. The bottom was a flat PMMA plate used as a supporter. However, filter paper in the thickness of several hundreds of micro

meters was hardly intimately contact with the hard PMMA mask even the assembly of top PMMA mask-middle filter paper-bottom PMMA plate was tightly clamped. This caused corona leakage from the edge of the stenciled wall of the mask to the masked region of the paper, leading to significant expansion of channel width and non-smooth channel borders. To solve the problem, an elastic PDMS pad was laid on the bottom PMMA plate. When the paper sheet was sandwiched by the three-layer mould complex as shown in Fig.1 c and tightly clamped, the paper sheet could intimately contact with the mask. Therefore, corona leakage no longer occurred, and the dimensions of the prepared channels were the same as designed.

### 3.1.2 The Time Period of Corona Discharge Treatment

The effect of corona discharge treating time on the hydrophilicity of the treated OTS-paper was studied by measuring water contact angles (WCAs) on the OTS-paper before and after the paper sheets (size:  $1 \times 3 \text{ cm}^2$ ) were exposed to corona discharge for varied time periods. As shown in Fig. 2, the WCAs decreased sharply from  $135.2 \pm 1.2^\circ$  to  $0^\circ$  with the increase of corona discharge treating time from 0 to 30 s. Thus, it means that a  $10 \text{ s cm}^{-2}$  corona discharge treating strength could turn the OTS-paper from hydrophobic to hydrophilic. Compared to our previous work<sup>10</sup> where UV lights were used to wettability-pattern the OTS-paper, the treating time was drastically reduced.

The thickness of hydrophilic layer was also measured after the OTS-paper sheets (size:  $1 \times 0.5 \text{ cm}^2$ ) were exposed to corona discharge for varied time periods. After corona discharge treatment, deionized water colored by green food dye was applied into the paper sheets and allowed air dry for 5 min. Then the dyed paper sheets were cut with a knife to show the smooth cross sections (see Fig. 3a, the thickness of green-colored layer was measured as the thickness of hydrophilic layer. The white layer was hydrophobic and prevented liquid from penetrating through the entire paper thickness). Fig. 3b shows that the thickness of hydrophilic layer increased with the increase of corona discharge treating time until leveled off. Fig. 3b also indicated that the maximum depth corona could reach inside the OTS-paper was  $\sim 50 \mu\text{m}$  under the

experiment conditions.

### 3.1.3 Wettability-Patterning of Paper

Based on the study described in the above sections, a simple and quick method for  $\mu$ PADs fabrication was established by OTS silanization of filter paper followed by region-selective corona discharge treatment. Water penetration could be well defined within the corona treated areas by the hydrophobic walls of OTS and the boundaries could be clearly observed (see Fig. 4). These results demonstrated the feasibility of using the technique of corona discharge treatment to fabricate hydrophilic-hydrophobic contrast on OTS-paper.

### 3.1.4 Stability

The stability of hydrophilic property in corona treated area was evaluated by measuring the WCAs on the surface of corona treated OTS-paper after storage in a dryer for varying time. The result (see Fig. S-1, available in ESI) showed that the hydrophilicity remained the same as its initial status after its storage for one month.

### 3.1.5 Mechanism Study

The mechanism of hydrophilic to hydrophobic conversion of filter paper after OTS coating has been reported in our previous work.<sup>10</sup> Here, discuss was focused on the mechanism of hydrophobic to hydrophilic conversion of OTS-paper after corona discharge treatment and on the differences between the present fabrication method and the one of our previous work.<sup>10</sup> Thus, spectroscopic analyses of X-ray photoelectron spectroscopy (XPS) and attenuated total reflectance Fourier transform-infrared (ATR-FT-IR) spectroscopy were conducted. XPS analyses revealed that O/C ratio of corona treated OTS-paper (0.78) was much higher than that of OTS-paper (0.19) (see Fig. S-2, available in ESI). This implied that oxygen-rich moieties had been introduced into the surface of OTS-paper after corona discharge treatment. ATR-FT-AR spectra further confirmed the deduction. Compared to the ATR-FT-AR spectrum of OTS-paper, peaks at 2916/cm and 2851/cm, which

corresponded to the asymmetric and symmetric stretching of  $-\text{CH}_2-$  group in the long alkyl chains of OTS, disappeared in the spectrum of corona treated OTS-paper (see Fig. S-3c, available in ESI). Meanwhile, the  $\text{C}=\text{O}$  stretching of carbonyl groups at  $\sim 1723/\text{cm}$  showed up in the spectrum of corona treated OTS-paper (see Fig. S-3c, available in ESI). This indicated that long alkyl chains of OTS coupling to paper cellulose had been decomposed and oxygen-contained polar groups were introduced into the surface of OTS-paper during corona discharge treatment, resulting in hydrophobic to hydrophilic conversion. It is noticed that the characteristic peaks of cellulose at 1160、1110、1056、1023  $/\text{cm}$  still existed after corona discharge treatment. This was quite different from the spectrum observed with  $\text{UV}/\text{O}_3$  treated OTS-paper, where all these characteristic peaks of cellulose disappeared.<sup>10</sup> It indicated that corona discharge treatment was a mild technique compared to  $\text{UV}/\text{O}_3$  technique, the latter decomposed not only long alkyl chains of OTS but also the skeleton structures of cellulose, consequently, turned the paper from white to yellow-dish. This was the reason why the limit of detection was significantly lowered when the  $\mu\text{PADs}$  fabricated by the present method were used in colorimetric analysis.

### 3.2 Nitrite Assay in Saliva Sample

Saliva contains components derived from serum<sup>34</sup> and can be collected more easily and noninvasively than blood. Therefore, saliva has been suggested to be a good alternative to blood for diagnostic purposes. Saliva nitrite has been reported to be a useful biomarker for real-time monitoring of dialysis progression.<sup>34, 35</sup>

To exploit the  $\mu\text{PADs}$  fabricated by the present technique to clinical diagnosis, colorimetric test of saliva nitrite was conducted on the prepared  $\mu\text{PADs}$ . A flower-shaped channel network with eight detection zones was chosen as the device design to perform multi-sample assays simultaneously and under the same condition. Fig. 5a shows the scanned image of a color-developed  $\mu\text{PAD}$  with one detection zone for blank control and seven detection zones for serially diluted  $\text{NO}_2^-$ . A calibration curve was constructed based on the color intensities of seven detection zones as shown in Fig. 5b. The dynamic linear range for  $\text{NO}_2^-$  was 20-160  $\mu\text{mol L}^{-1}$  (linear

regression equation:  $y=12123x-151.7$ ,  $x$  for  $\text{NO}_2^-$  concentration at millimolar,  $y$  for the color intensity; correlation coefficient: 0.9927). The limit of detection defined as the concentration equivalent to 3-folds of standard deviation of color intensities for 3 blank samples was  $7.8 \mu\text{mol L}^{-1}$ , which was lowered by an order of magnitude compared to our previous work.<sup>10</sup> This was due to the corona discharge treated paper in the present work remained colorless while the UV/O<sub>3</sub>-treated paper in the previous work turned slightly yellowish, which resulted in relatively high blank background.

The  $\text{NO}_2^-$  content in saliva sample determined by the proposed method was  $68.5 \pm 5.1 \mu\text{mol L}^{-1}$  ( $n=3$ ), which agreed well with the concentration of  $69.7 \pm 0.2 \mu\text{mol L}^{-1}$  ( $n=3$ ) determined by ion chromatography. This result demonstrates the feasibility of  $\mu\text{PADs}$  fabricated by the proposed method to be a simple and inexpensive approach for de-centralized clinical diagnosis.

### 3.3 Fluids Control on the $\mu\text{PAD}$ via On-site Corona discharge treatment

Since the hydrophilization of OTS-paper could be quickly conducted on-site with a hand-held corona generator, it would be possible to prepare a type of single-use 'on' valves in  $\mu\text{PADs}$ . The valve was designed as a 1 mm wide hydrophobic dam at the end of a channel where the fluid should be temporally stopped. At the moment when the blocked fluid needed to move forward, the valve could be quickly open via targeted corona discharge, then fluid could flow forward again via capillary wicking. To test the feasibility of the proposed single-use 'on' valves, a programmed acid-base neutralization process was designed as the model for fluid control, and the  $\mu\text{PAD}$  shown in Fig. 6a was fabricated for the test. The device consisted of two sample reservoirs (S1 for basic solution and S2 for acid solution), one reaction cell (R), and two single-use 'on' valves (V1, V2) that were positioned at the ends of basic and acid channels, respectively. With such a device, both the acid solution and the basic solution can be programmed to enter the reaction cell by sequentially opening the valves via on-site targeted corona discharge treatment. In order to visualize clearly the results of the programmed acid-base reaction, a small quantity of acid-base indicator

(phenolphthalein) solution was applied into the reaction cell. NaOH and HCl solutions were then introduced into sample reservoirs S1 and S2, respectively (Fig. 6a). Both the acid and alkaline solutions were driven forward along the channels by capillary wicking until they were blocked by the closed valves. Afterwards, the electrode tip with soft corona was targeted to the valve V1 for 1 s (Fig. 6b), leading to the valve open. As a result, NaOH solution penetrated into the reaction cell, the phenolphthalein indicator in the cell gradually turning violet (Fig. 6c and Fig. 6d). Then same operation was done to open V2, consequently HCl solution entered into the reaction cell (Fig. 6e). HCl solution neutralized NaOH solution in the cell. Thus, the alkaline medium in the cell was gradually transformed to acidic, and violet color of indicator faded (Fig. 6f and Fig. 6g). A video recording the whole process was given in ESI. This programmed acid-base reaction model demonstrated that the closed wettability-switching valves can be instantaneously opened by targeted corona discharge and that an array of such single-use 'on' valves can be easily integrated in the channel network to perform complicated fluid control in the  $\mu$ PADs.

#### 4 Conclusion

This article has developed the technique for fabricating microfluidic paper-based analytical devices and on-device fluid control by using a hand-held corona generator. The established method features simplicity in operation, low in cost, and less in environmental pollution. Moreover, it allows analysts to fabricate  $\mu$ PADs in their own laboratories. The demonstrated simple approach for salivary nitrite analysis with the developed  $\mu$ PADs may be used as a noninvasive method for point of care tests. The targeted corona discharge can effectively open the wettability-switching valves, and the single-use 'on' valves can be easily integrated in the channel network to perform complicated fluid control in the  $\mu$ PADs, which will broaden the practical applications of  $\mu$ PADs for multi-step assays (for instance, immunoassays) that required sequential mixing of reagents and analytes.

## Acknowledgement

This work is funded by the National Natural Science Foundation of China (Project No. 20890020) and the National Science & Technology Supporting Program of China (Grant 2012BAI13B06)

## References

1. A. W. Martinez, S. T. Phillips, M. J. Butte and G. M. Whitesides, *Angew. Chem., Int. Ed. Engl.*, 2007, **46**, 1318-1320.
2. D. D. Liana, B. Raguse, J. J. Gooding and E. Chow, *Sensors*, 2012, **12**, 11505-11526.
3. D. M. Cate, J. A. Adkins, J. Mettakoonpitak and C. S. Henry, *Anal. Chem.*, 2015, **87**, 19-41.
4. X. Li, D. R. Ballerini and W. Shen, *Biomicrofluidics*, 2012, **6**, 11301-1130113.
5. Y. Jiang, C. Ma, X. Hu and Q. He, *Progr. Chem.*, 2014, **26**, 167-177.
6. X. Chen, J. Chen, F. Wang, X. Xiang, M. Luo, X. Ji and Z. He, *Biosens. Bioelectron.*, 2012, **35**, 363-368.
7. S. Ge, L. Ge, M. Yan, X. Song, J. Yu and J. Huang, *Chem. Commun.*, 2012, **48**, 9397-9399.
8. L. Ge, S. Wang, X. Song, S. Ge and J. Yu, *Lab Chip*, 2012, **12**, 3150-3158.
9. X. Hu, L. Lu, C. Fang, B. Duan and Z. Zhu, *J. Agric. Food Chem.*, 2015, DOI: 10.1021/acs.jafc.5b04530.
10. Q. He, C. Ma, X. Hu and H. Chen, *Anal. Chem.*, 2013, **85**, 1327-1331.
11. P. D. Haller, C. A. Flowers and M. Gupta, *Soft Matter*, 2011, **7**, 2428-2432.
12. E. Carrilho, A. W. Martinez and G. M. Whitesides, *Anal. Chem.*, 2009, **81**, 7091-7095.
13. Y. Lu, W. Shi, L. Jiang, J. Qin and B. Lin, *Electrophoresis*, 2009, **30**, 1497-1500.
14. Y. Lu, W. Shi, J. Qin and B. Lin, *Anal. Chem.*, 2009, **82**, 329-335.
15. T. Songjaroen, W. Dungchai, O. Chailapakul and W. Laiwattanapaisal, *Talanta*, 2011, **85**, 2587-2593.
16. P. de Tarso Garcia, T. M. G. Cardoso, C. D. Garcia, E. Carrilho and W. K. T. Coltro, *RSC Adv.*, 2014, **4**, 37637-37644.
17. W. Dungchai, O. Chailapakul and C. S. Henry, *Analyst*, 2011, **136**, 77-82.
18. X. Li, J. Tian, T. Nguyen and W. Shen, *Anal. Chem.*, 2008, **80**, 9131-9134.
19. X. Li, J. Tian, G. Garnier and W. Shen, *Colloids Surf., B*, 2010, **76**, 564-570.
20. C. Xu, L. Cai, M. Zhong and S. Zheng, *RSC Adv.*, 2015, **5**, 4770-4773.
21. K. Abe, K. Suzuki and D. Citterio, *Anal. Chem.*, 2008, **80**, 6928-6934.
22. K. Abe, K. Kotera, K. Suzuki and D. Citterio, *Anal. Bioanal. Chem.*, 2010, **398**, 885-893.
23. J. Nie, Y. Zhang, L. Lin, C. Zhou, S. Li, L. Zhang and J. Li, *Anal. Chem.*, 2012, **84**, 6331-6335.
24. J. Olkkonen, K. Lehtinen and T. Erho, *Anal. Chem.*, 2010, **82**, 10246-10250.
25. G. Chitnis, Z. Ding, C.-L. Chang, C. A. Savran and B. Ziaie, *Lab Chip*, 2011, **11**, 1161-1165.
26. L. Cai, Y. Wang, Y. Wu, C. Xu, M. Zhong, H. Lai and J. Huang, *Analyst*, 2014, **139**, 4593-4598.
27. H. Noh and S. T. Phillips, *Anal. Chem.*, 2010, **82**, 8071-8078.
28. A. W. Martinez, S. T. Phillips, Z. Nie, C. M. Cheng, E. Carrilho, B. J. Wiley and G. M. Whitesides, *Lab Chip*, 2010, **10**, 2499-2504.
29. K. Haubert, T. Drier and D. Beebe, *Lab Chip*, 2006, **6**, 1548-1549.

30. L. A. Filla, D. C. Kirkpatrick and R. S. Martin, *Anal. Chem.*, 2011, **83**, 5996-6003.
31. R. T. Davies, D. Kim and J. Park, *J. Micromech. Microeng.*, 2012, **22**, 055003.
32. X. Li, J. Tian and W. Shen, *Anal. Bioanal. Chem.*, 2010, **396**, 495-501.
33. Y. Tanaka, N. Naruishi, H. Fukuya, J. Sakata, K. Saito and S.-i. Wakida, *J. Chromatogr. A*, 2004, **1051**, 193-197.
34. T. M. Blicharz, D. M. Rissin, M. Bowden, R. B. Hayman, C. DiCesare, J. S. Bhatia, N. Grand-Pierre, W. L. Siqueira, E. J. Helmerhorst, J. Loscalzo, F. G. Oppenheim and D. R. Walt, *Clin. Chem.*, 2008, **54**, 1473-1480.
35. S. A. Klasner, A. K. Price, K. W. Hoeman, R. S. Wilson, K. J. Bell and C. T. Culbertson, *Anal. Bioanal. Chem.*, 2010, **397**, 1821-1829.

## Figure Captions

**Fig. 1** Schematic diagram for the fabrication of  $\mu$ PADs: (a) the native filter paper; (b) the OTS-coated paper; (c) the OTS-coated paper sheet was sandwiched between the top PMMA mask and the middle PDMS soft pad of the mould complex. After the assembly was tightly clamped, it was exposed to corona discharge; (d) the  $\mu$ PAD with hydrophilic-hydrophobic patterns (the white area was hydrophilic while the blue area was hydrophobic).

**Fig. 2** The water contact angles measured on the OTS-Paper after the paper were exposed to corona discharge with varied time periods. The size of paper sheets:  $1 \times 3 \text{ cm}^2$ .  $n=9$

**Fig. 3** (a) Microscopic image of the cross-section of the OTS-paper that was corona discharge treated for 40 s. (b) The thickness of hydrophilic layer after the OTS-paper sheets (size:  $1 \times 0.5 \text{ cm}^2$ ) were exposed to corona discharge for varied time periods.

**Fig. 4** Hydrophilic–hydrophobic contrasts: (a) each pattern was subjected to corona discharge for 45 s, then a drop of dye solution ( $5 \text{ }\mu\text{L}$ ) of different colors was applied into the central reagent zones of each pattern, respectively; (b) each dot on the OTS-paper was treated for 5 s, then aliquots of  $0.5 \text{ }\mu\text{L}$  differently-colored dye solutions were pipetted into the treated dots.

**Fig. 5** Colorimetric assays of saliva nitrite with  $\mu$ PADs fabricated by the proposed method: (a) scanned image of a color-developed  $\mu$ PAD. The  $\text{NO}_2^-$  concentration deposited in 0~7 detection zones was 0, 0.02, 0.04, 0.08, 0.16, 0.32, 0.64,  $1.28 \text{ mmol L}^{-1}$ , respectively; (b) the calibration curve constructed for  $\text{NO}_2^-$  concentrations mentioned in (a)

**Fig. 6** Programmed acid-base neutralization on a  $\mu$ PAD with wettability-switching valves : (a) layout of the channel network on the  $\mu$ PAD. S1, reservoir for NaOH solution; S2, reservoir for HCl solution; V1 and V2, wettability-switching valves; R, reaction cell where phenolphthalein indicator solution was applied; (b) corona discharge was targeted to V1 for 1 s, leading to V1 being opened; (c) left half area of the reaction cell turned violet after V1 had been opened for 3 s; (d) the whole reaction

cell became violet after V1 had been opened for 30 s; (e) corona discharge was targeted to V2 for 1 s, resulting in V2 valve being opened; (f) violet color in the right half area of reaction cell faded after V2 had been opened for 1 min; (g) violet color in the whole reaction cell faded after V2 had been opened for 3 min.

Fig. 1

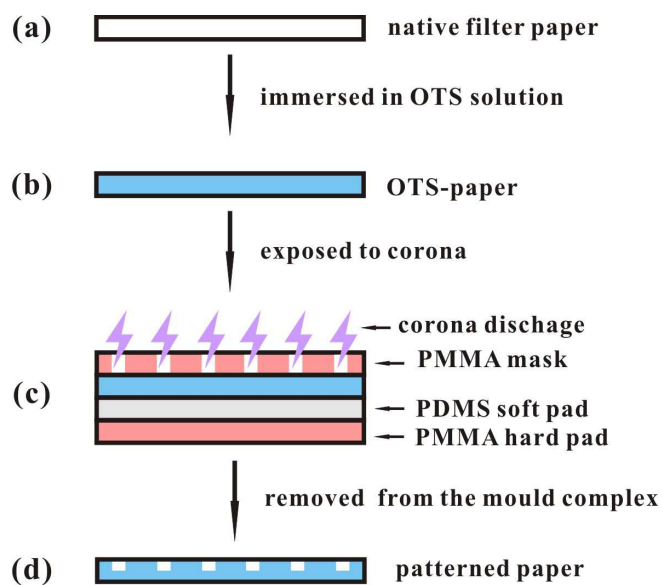


Fig. 2

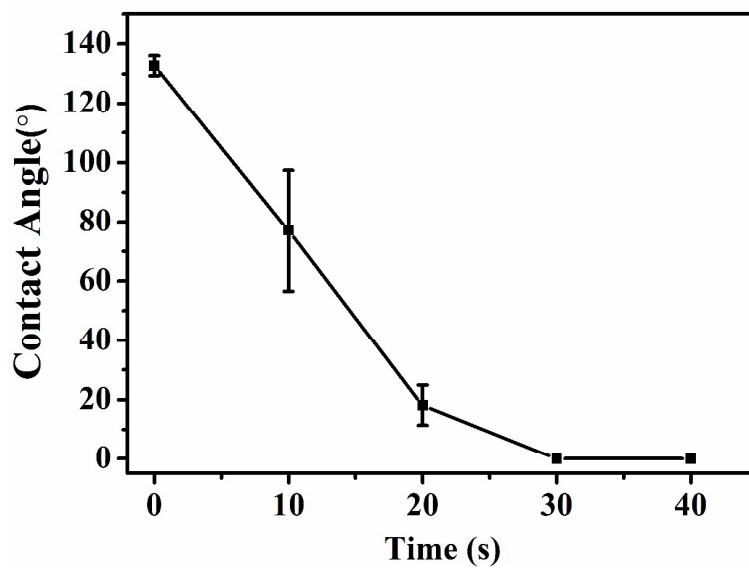
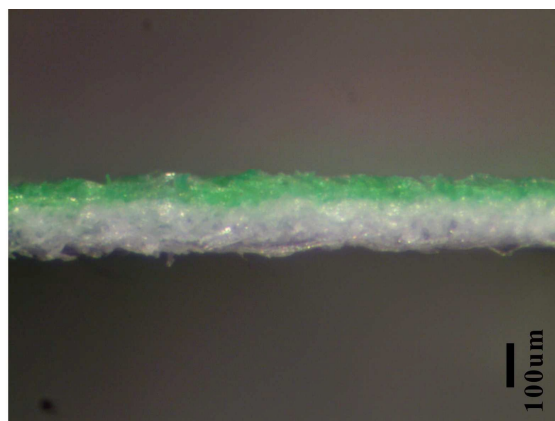
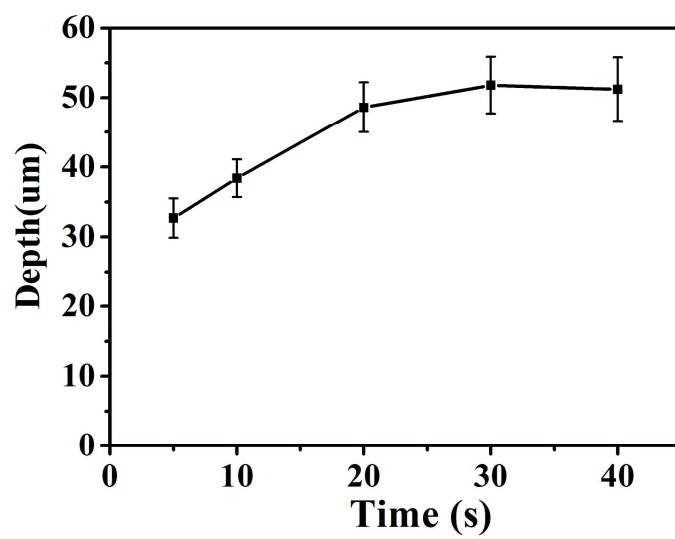


Fig. 3

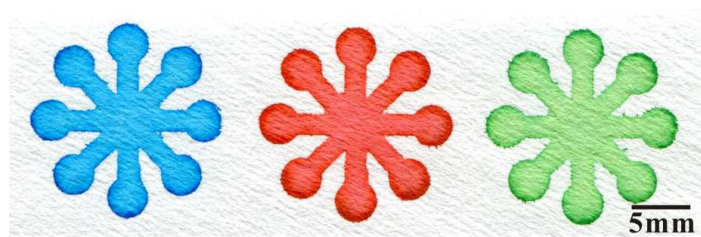


(a)

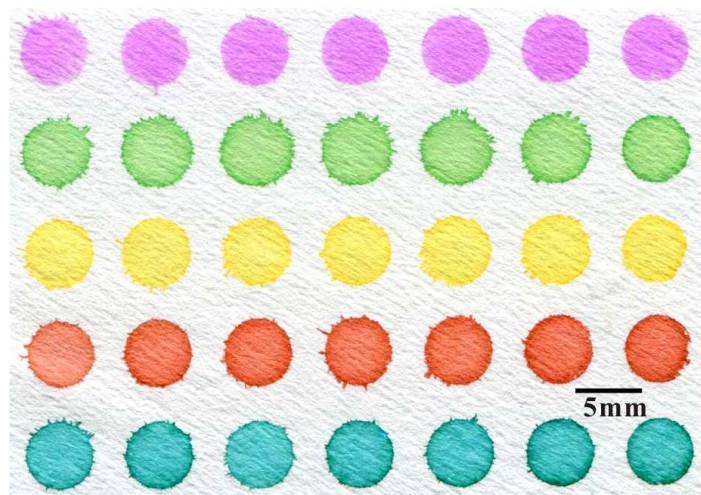


(b)

Fig. 4

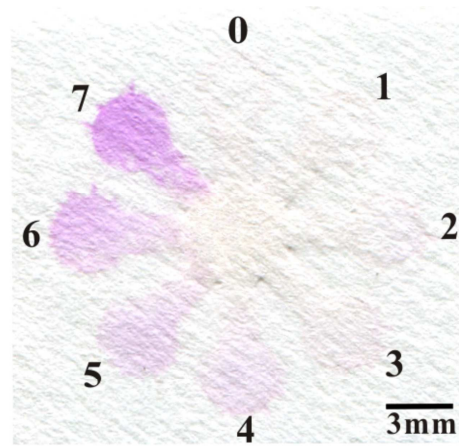


(a)

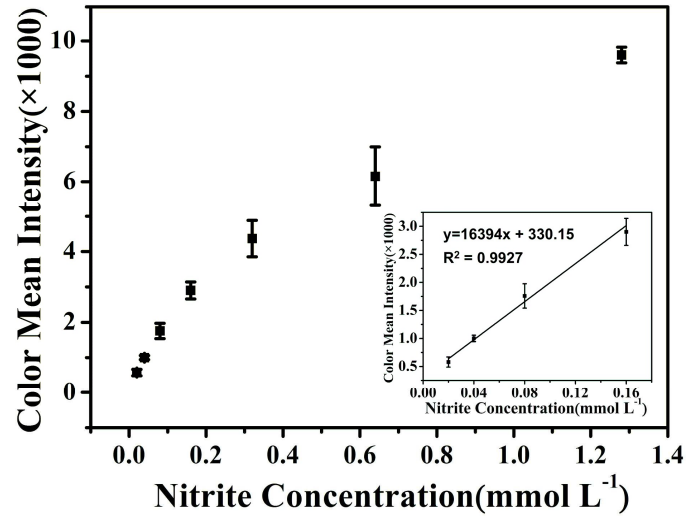


(b)

Fig. 5

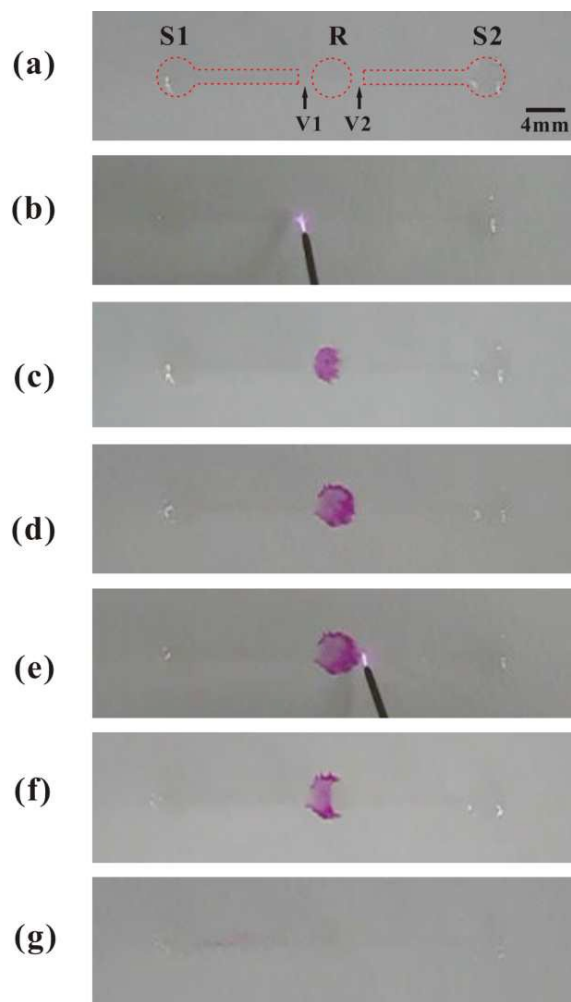


(a)



(b)

Fig. 6



A simple method for fabrication of microfluidic paper-based analytical devices and on-device fluid control with a portable corona generator was developed.

